

# EVOLUTION OF MAGNETIC AND SUPERCONDUCTING FLUCTUATIONS WITH DOPING OF HIGH- $T_c$ SUPERCONDUCTORS (An electronic Raman scattering study)

G. BLUMBERG<sup>1,2,3,†</sup> M.V. KLEIN<sup>1,2</sup> K. KADOWAKI<sup>4</sup> C. KENDZIORA<sup>5</sup> P. GUPTASARMA<sup>1,6</sup> and D. HINKS<sup>1,6</sup>

<sup>1</sup>NSF Science and Technology Center for Superconductivity

<sup>2</sup>Department of Physics, University of Illinois at Urbana-Champaign, Urbana, IL 61801-3080

<sup>3</sup>Institute of Chemical Physics and Biophysics, R vala 10, Tallinn EE0001, Estonia

<sup>4</sup>Institute of Materials Science, University of Tsukuba, Tsukuba, Ibaraki 305, Japan

<sup>5</sup>Code 6653, Naval Research Laboratory, Washington, D.C. 20375

<sup>6</sup>Materials Science Division, Argonne National Laboratory, Argonne, IL 60439

**Abstract**—For  $\text{YBa}_2\text{Cu}_3\text{O}_{6+\delta}$  and  $\text{Bi}_2\text{Sr}_2\text{CaCu}_2\text{O}_{8\pm\delta}$  superconductors, electronic Raman scattering from high- and low-energy excitations has been studied in relation to the hole doping level, temperature, and energy of the incident photons. For underdoped superconductors, it is concluded that short range antiferromagnetic (AF) correlations persist with hole doping and doped single holes are incoherent in the AF environment. Above the superconducting (SC) transition temperature  $T_c$  the system exhibits a sharp Raman resonance of  $B_{1g}$  symmetry and about 75 meV energy and a pseudogap for electron-hole excitations below 75 meV, a manifestation of a partially coherent state forming from doped incoherent quasi-particles. The occupancy of the coherent state increases with cooling until phase ordering at  $T_c$  produces a global SC state.

## I. INTRODUCTION

The normal and superconducting (SC) properties of doped cuprate high-temperature superconductors are very different from those of conventional metals and are usually viewed as manifestations of strong electron-electron correlations. These correlations cause the antiferromagnetic (AF) state in the undoped cuprates. The SC coherence length,  $\xi_{SC}$ , is of the order of a few lattice spacings, considerably shorter than in conventional superconductors. The persistence of short-range AF correlations with doping has been thought to lead to an effective pairing mechanism and to the unconventional normal state properties [1].

The underdoped SC cuprates have low carrier density. The mean free path of the holes is shorter than their de Broglie wavelength which brings the underdoped cuprates into a class of “bad metals” [2]. For cuprates a rough estimate of parameter  $k_F\xi_{SC}$  ( $k_F$  is Fermi wave vector) lead to values of about 3 to 20, two orders of magnitude smaller than for conventional Bardeen-Cooper-Schrieffer (BCS) superconductors. It was shown by Uemura *et. al.* [3] that, for cuprates, the SC transition occurs around the temperature at which the thermal de Broglie wavelength of the pairs is 2 to 6 times greater than the average interpair separation. A pair size comparable to the average interparticle spacing  $k_F^{-1}$  brings

cuprates to an intermediate regime between the BCS limit of large overlapping Cooper pairs ( $k_F\xi_{SC} \gg 1$ ) and of Bose-Einstein (BE) condensation of composite bosons ( $k_F\xi_{SC} \ll 1$ ) consisting of tightly bound fermion pairs [3,4]. As a consequence of the low carrier density and the short SC correlation length the transition to the SC state may not display a typical BCS behavior. In the underdoped cuprates,  $T_c$  may be strongly suppressed with respect to the pairing temperature and be determined by phase fluctuations [5,6].

## II. PROBING MAGNETIC AND SUPERCONDUCTING FLUCTUATIONS BY ELECTRONIC RAMAN SCATTERING

Electronic Raman scattering is a local high-energy probe for both (i) the short-range AF correlations and (ii) the SC order parameter in doped, SC samples through excitation across the SC gap.

Two-magnon (2-M) Raman scattering directly probes short-wavelength magnetic fluctuations, which may exist without long-range AF order [7,8]. The Raman process takes place through a photon-stimulated virtual charge-transfer (CT) excitation that exchanges two Cu spins. This process may also be described as creation of two interacting magnons. The CT excitation is the same one which virtually produces the spin superexchange con-

stant  $J$ . In the AF environment with a correlation length  $\xi_{AF}$  covering 2 to 3 lattice constants, the spin exchange process requires an energy of about  $3J$ . The magnetic Raman scattering peak position, intensity, and shape provide information about fluctuations in a state of short-range AF order [8].

Electronic Raman scattering by charge fluctuations in metals arises from electron-hole (e-h) excitations near the Fermi surface (FS). For a normal Fermi liquid model of the cuprates, the scattering would have finite intensity only at very low frequencies. For strongly correlated systems, incoherent quasi-particle (QP) scattering leads to finite Raman intensity over a broad region of frequency [9,10], and the intensity can be used as a measure of the incoherent scattering. Indeed, for the cuprates in the normal state, an almost frequency independent Raman continuum has been observed that extends to at least 2 eV [8,11,12]. In the SC state of optimally and overdoped cuprates, the low-frequency tail of the Raman continuum changes to reflect the SC effects. The opening of a SC gap reduces the incoherent inelastic scattering processes and reduces the strength of the continuum. Freed from the heavy damping, the QPs now show a gap in their spectral function. Thus, the electronic Raman spectrum of e-h-pair excitations acquires the so-called  $2\Delta$ -peak due to gap excitations,  $2\Delta(\mathbf{k})$ , where  $\mathbf{k}$  is a wave vector on the FS. For optimally and overdoped cuprates, opening of an anisotropic superconducting gap,  $2\Delta(\mathbf{k})$ , in the e-h-pair excitation spectrum at wave vector  $\mathbf{k}$  causes suppression of the low-frequency part of the continuum due to both a gapped density of states and to a drop in the low-energy QP scattering rate. For underdoped cuprates, only a relatively weak peak has been observed within the strong Raman continuum [13]; its energy does not scale with sample  $T_c$ , and its origin has been unclear.

We studied both AF and SC correlations and found that for underdoped samples, the short-range AF correlations persist with hole doping. Furthermore, the presence of a Raman peak of  $B_{1g}$  symmetry at  $\sim 75$  meV is interpreted as evidence that incoherent doped holes form above  $T_c$  a long lived collective state with a sharp resonance of  $B_{1g}$  ( $d_{x^2-y^2}$ ) symmetry. The temperature dependence of this peak is evidence that this state gains phase coherence at  $T_c$  and participates in the collective SC state. Binding of incoherent QPs into the coherent state reduces the low-frequency scattering rate and leads to a pseudogap in the spectra.

### III. EXPERIMENTAL

The  $\text{YBa}_2\text{Cu}_3\text{O}_{6+\delta}$  and  $\text{Bi}_2\text{Sr}_2\text{CaCu}_2\text{O}_{8\pm\delta}$  single crystals were grown and postannealed as described in Refs. [14–19]. Raman measurements were made using systems described in Refs. [12,20]. The polarization of the incoming and outgoing light with respect to the copper-

oxygen plane is shown by the long straight arrows in Fig. 1. It gives mainly Raman spectra of  $B_{1g}$  symmetry. For magnetic excitations, the  $B_{1g}$  scattering channel couples to pairs of short wavelength magnons near the magnetic Brillouin zone boundary [8]. For the e-h excitations near the FS, the Raman form-factor for  $B_{1g}$  symmetry is peaked for  $\mathbf{k}$  near the antinode wave vectors  $\{\mathbf{k}_{an}\} = \{(0, \pm \frac{\pi}{a}) \text{ and } (\pm \frac{\pi}{a}, 0)\}$  [21], where the anisotropic SC gap magnitude is believed to reach its maximum value  $\Delta_{max}$ . Indeed, the  $B_{1g}$  scattering geometry reveals interesting excitations in both magnetic and e-h excitation channels.

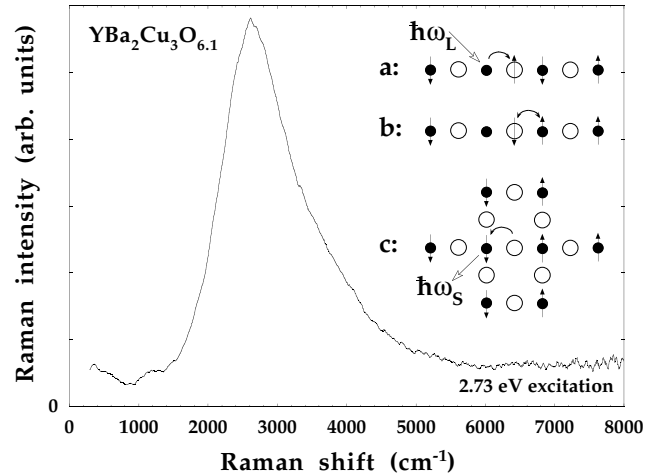


FIG. 1. Two-magnon Raman scattering spectra from  $\text{YBa}_2\text{Cu}_3\text{O}_{6.1}$  AF insulator at room temperature. Inset illustrates the photon induced spin superexchange mechanism for Raman scattering and shows the polarization of the incoming laser light and the outgoing scattered light (long, straight arrows) with respect to the copper (solid circles) - oxygen (open circles) plane.

### IV. ANTIFERROMAGNETIC CORRELATIONS

Figures 1 and 2 show the high-energy part of  $B_{1g}$  electronic Raman scattering spectra at room temperature as a function of hole doping. The typical spectrum from the AF insulator exhibits a strong band assigned to scattering by 2-Ms, that is the photon-induced superexchange of two spins on two nearest neighbor Cu  $3d^9$ -orbital sites through the intervening 2p-oxygen orbital. The incoming photon can cause a charge (hole) transfer from the  $3d^9 2p^6$  to  $3d^{10} 2p^5$  configuration (Fig. 1a). The probability of the virtual intermediate CT process is expected to be resonantly enhanced when the incoming photon energy  $\hbar\omega_L$  approaches the Cu 3d – O 2p CT energy  $E_{CT}$  [8,22]. In the next step (Fig. 1b) a  $2p^5$  and  $3d^9$  spin exchange occurs, and in the last step (Fig. 1c) the charge returns to the initial Cu  $3d^9$  orbital and emits an inelastically scattered photon  $\hbar\omega_S = \hbar\omega_L - \hbar\omega_{2M}$ . As a result of the superexchange, each of two exchanged spins sees three fer-

romagnetically aligned neighbors, at a cost of  $\sim 3J$  due to the Heisenberg interaction energy  $J \sum_{\langle i,j \rangle} (\mathbf{S}_i \cdot \mathbf{S}_j - \frac{1}{4})$  [ $\mathbf{S}_i$  is the spin on site  $i$  and the summation is over near-neighbor Cu pairs.]. Thus for the AF insulators, the 2-M peak position yields an estimate of  $J \approx 125$  meV.

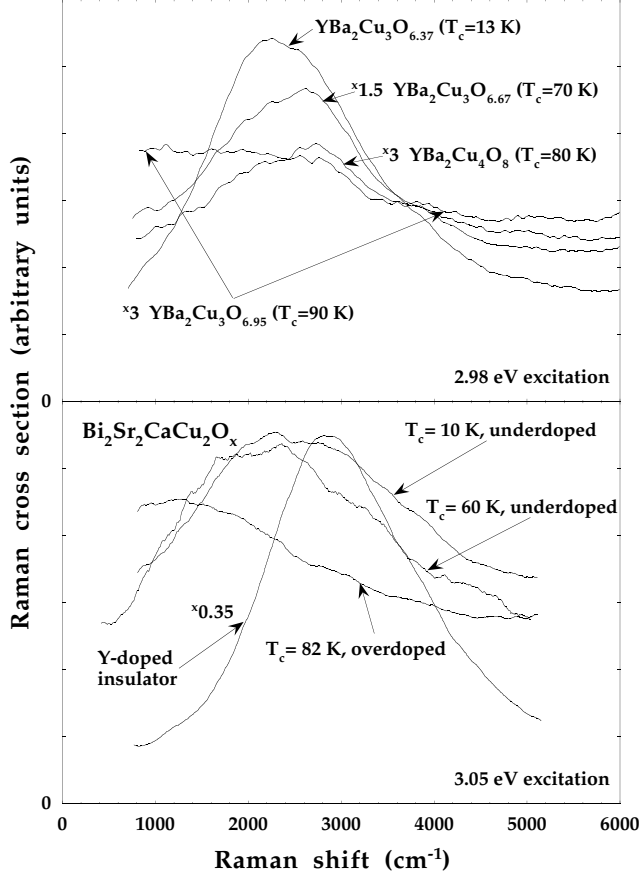


FIG. 2. The  $B_{1g}$  continuum and two-magnon Raman scattering spectra at room temperature as a function of doping for  $\text{YBa}_2\text{Cu}_3\text{O}_{6+\delta}$  and  $\text{Bi}_2\text{Sr}_2\text{CaCu}_2\text{O}_{8\pm\delta}$ .

For doped superconductors, the spectra (Fig. 2) exhibit a background continuum plus a broad peak, which, similar to the AF case, has been assigned to the double spin-flip excitation in the short-range AF environment. For the process of two-spin superexchange to require the full  $3J$  energy cost, spins on six further Cu neighbor sites must show AF alignment. The doped holes are believed to form singlets with the holes that would otherwise form local AF order [23]. This screens the effective spin moment on the doped Cu site and might lead to reduction of the spin superexchange energy in the vicinity of holes. With doping, as is seen from Fig. 2, the 2-M scattering peak broadens, weakens, and shifts to lower frequency. The existence of the peak in the SC cuprates indicates persistence of a local short-range AF order extending a few lattice spacings.

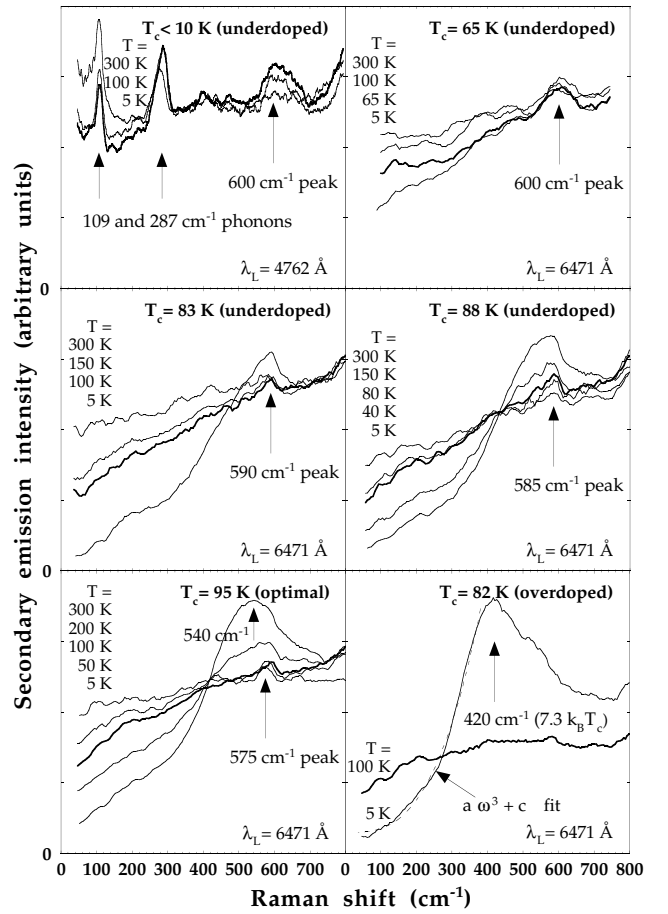


FIG. 3. The low-energy portion of  $B_{1g}$  Raman scattering spectra for  $\text{Bi}_2\text{Sr}_2\text{CaCu}_2\text{O}_{8\pm\delta}$  as a function of temperature and doping.

## V. INCOHERENT CONTINUUM, PSEUDOGAP AND RESONANT EXCITATION AT 75 MEV

Figure 3 shows the low-energy  $B_{1g}$  Raman scattering spectra for  $\text{Bi}_2\text{Sr}_2\text{CaCu}_2\text{O}_{8\pm\delta}$  superconductors as function of temperature and doping. The most prominent feature of the spectra is the electronic continuum. According to the existing phenomenology for the continuum [9,24] and allowing for the symmetry of the  $B_{1g}$  Raman form factor, we believe the  $B_{1g}$  Raman continuum intensity,  $I(\omega, T)$ , to be proportional to the incoherent QP inverse lifetime  $\tau_{\{\mathbf{k}_{an}\}}^{-1}(\omega, T) = \Gamma_{\{\mathbf{k}_{an}\}}(\omega, T) \approx \sqrt{(\alpha\omega)^2 + (\beta T)^2}$  for  $\mathbf{k}$  in the vicinity of wavevectors  $\{\mathbf{k}_{an}\}$ :  $I(\omega, T) \propto [1 + n(\omega, T)]\omega\Gamma/(\omega^2 + \Gamma^2)$ , where  $n(\omega, T)$  is the Bose factor,  $\alpha$  and  $\beta$  are phenomenological parameters of order unity. The continuum extends to a few electron-volts. For higher temperatures it starts from very low frequencies, affirming strong incoherent scattering even for low lying e-h excitations.

Cooling the underdoped samples gradually strengthens a remarkably sharp scattering peak at about  $600 \text{ cm}^{-1}$

(75 meV). For underdoped  $\text{YBa}_2\text{Cu}_3\text{O}_{6.6}$  a similar excitation has been first observed by F. Slakey *et al.* [13]. The integrated (above the continuum line) intensity of the peak contains just a few per cent of the integrated 2-M scattering intensity. This peak has  $B_{1g}$  symmetry and is not present for other geometries. The peak position shows little temperature or doping dependence. Below  $T_c$  the peak undergoes further intensity enhancement, turning into  $2\Delta$ -peak at higher dopings.

The narrow width of the  $600\text{ cm}^{-1}$  peak in the Raman spectra ( $\Gamma_{\text{peak}} \lesssim 50\text{ cm}^{-1}$ ) is more than an order of magnitude smaller than the inverse QP lifetime  $\Gamma_{\{\mathbf{k}_{an}\}}(600\text{ cm}^{-1}, T)$  associated with the continuum. The two very different lifetimes for the  $600\text{ cm}^{-1}$  mode and the continuum suggest that we are essentially dealing with a two component system: A spectroscopically well defined, long lived,  $600\text{ cm}^{-1}$  mode on top of the strong incoherent background.

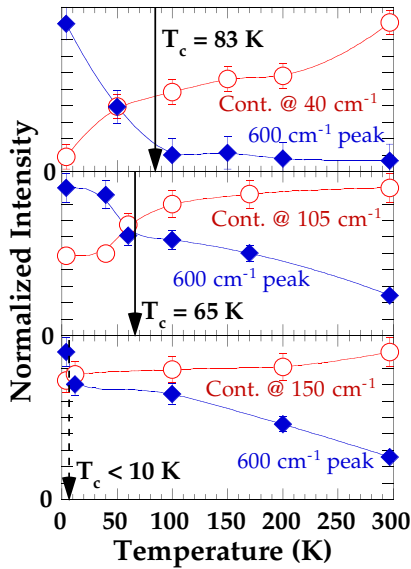


FIG. 4. The temperature dependence of the normalized low-frequency continuum intensity (circles) and a normalized integrated above the continuum  $600\text{ cm}^{-1}$  peak intensity (diamonds) for the  $T_c < 10\text{ K}$ , 65 and 83 K underdoped samples. Vertical arrows denote  $T_c$ .

In Fig. 4 we plot the temperature dependence of the integrated above the continuum line intensity of the  $600\text{ cm}^{-1}$  mode for the three underdoped samples with  $T_c < 10\text{ K}$ , 65 and 83 K. We also plot the temperature dependence of the low-frequency continuum intensity. The integrated intensity of the  $600\text{ cm}^{-1}$  mode smoothly increases with cooling until the temperature reaches  $T_c$  where the intensity shows a sudden enhancement. With cooling, the low-frequency portion of the continuum simultaneously shows an intensity reduction. The intensity reduction is an indication of a drop in the low-frequency ( $\omega < 600\text{ cm}^{-1}$ ) inverse lifetime  $\tau_{\{\mathbf{k}_{an}\}}^{-1}(\omega, T)$ . The sup-

pression of the low-frequency spectral weight in Raman spectra is similar to the pseudogap phenomena that has been observed in spin-excitation spectra [25,26], as well as in optical [27], ARPES [17,28] and tunneling [29] studies.

## VI. SUPERCONDUCTING FLUCTUATIONS ABOVE $T_c$ AND COHERENCE OF THE ELECTRONIC SYSTEM

All of the properties observed by Raman, ARPES, IR, and tunneling spectroscopies reveal an increase in the coherence of the electronic system while the underdoped cuprates are cooled toward  $T_c$ . The rearrangement of the Raman spectra with formation of the 75 meV mode is an indication that a partially coherent state forms above  $T_c$  out of the incoherent QPs in the vicinity of  $\{\mathbf{k}_{an}\}$  points. This long-lived state might consist of bound states of doped holes (preformed Cooper pairs) or of more complex many-body objects. Light scattering may break up the bound state into unbound QPs by a process similar to 2-M scattering. We propose that this process enhanced by a final state resonance is the origin of the  $600\text{ cm}^{-1}$   $B_{1g}$  Raman peak and suggest that it should be present for underdoped materials with AF correlations sufficient to exhibit underdamped 2-M excitations. The AF correlations that cover a few lattice spacings should last at least for  $10^{-13}\text{ s}$ , the lifetime of the coherent state.

Occupancy of the coherent state lowers the density of the incoherent single holes, leading to reduction of the low-frequency inverse lifetime, suppression of the incoherent low-frequency density of states, and formation of the pseudogap. We note that because of different couplings to light and also because of the very different lifetimes of single holes and the bound state, there is no conservation of spectral weight for Raman scattering: the low-frequency intensity reduction is stronger than the increase of the intensity of the  $600\text{ cm}^{-1}$  mode. As seen from Fig. 3, the low-temperature reduction of the scattering rate, as also shown by optical data [27], occurs only below the  $600\text{ cm}^{-1}$  energy. Cooling increases the occupancy of the coherent state and enhances the pseudogap until phase ordering at  $T_c$  produces a global SC state. Simultaneously, due to the phasing effect, the Raman spectra acquire additional  $600\text{ cm}^{-1}$  peak intensity.

For the very underdoped sample ( $T_c < 10\text{ K}$ ), only a weak pseudogap develops, and the integrated  $600\text{ cm}^{-1}$  peak intensity exhibits a weak enhancement (see Fig. 4). Both the pseudogap and the peak enhancement are stronger for the  $T_c = 65\text{ K}$  sample. The sample with higher doping ( $T_c \geq 83\text{ K}$ ) exhibits an effective condensation into the SC state with formation of a  $2\Delta$ -like feature in the Raman spectra out of the  $600\text{ cm}^{-1}$  peak. We note also that for all underdoped samples, only a partial

condensation of single holes in the SC state occurs even at the lowest temperature.

The coherent excitation near  $600\text{ cm}^{-1}$  above  $T_c$  weakens with doping. Instead, a strong coherent  $2\Delta$ -peak, much stronger than the  $600\text{ cm}^{-1}$  peak for the underdoped materials, develops below  $T_c$ . For the overdoped sample, the  $2\Delta$ -peak shape, including its low-frequency tail, may be reproduced by Fermi-liquid based Raman scattering theory for  $d$ -wave SC with a large FS that predicts a cubic power law for the low-frequency tail of the  $B_{1g}$  scattering intensity [21]. This demonstrates that a large FS is restored for materials above the optimal doping and that at the higher dopings and low temperatures the incoherent scattering is greatly reduced up to about  $400\text{ cm}^{-1}$ .

## VII. CONCLUSIONS

Our analysis of a broad range of Raman data for cuprates at different dopings implies that for the underdoped superconductors:

- (i) Short-range AF order over a few lattice spacings persists upon doping from the AF insulator.
- (ii) Single quasi-particle excitations for  $\mathbf{k}$  in the vicinity of  $\{\mathbf{k}_{an}\}$  points are incoherent.
- (iii) In the presence of short range AF order, doped holes form long lived coherent state.
- (iv) Binding of holes in the coherent state reduces the incoherent low-frequency scattering rate and a pseudogap forms in the spectra.
- (v) The occupancy of the coherent state increases with cooling until phase ordering at  $T_c$  produces a global SC state.

For overdoped superconductors, short range magnetic excitations become overdamped, no coherent QP excitations are observed above  $T_c$ , a strong coherent  $2\Delta$ -peak corresponding to the excitations across the superconducting gap develops below  $T_c$ .

We benefit by discussions with D.N. Basov, A.V. Chubukov, V.J. Emery, S.A. Kivelson, P. Lee, D.K. Morr, D. Pines, P.M. Platzman and Y.J. Uemura. We are grateful to B. Dabrowski, W.C. Lee, and B.W. Veal for samples. The work was supported by NSF grant DMR 93-20892 (GB, MVK), NSF cooperative agreement DMR 91-20000 through the STCS (GB, MVK, PG, DH), ONR (CK), and DOE-BES contract W-31-109-ENG-38 (PG, DH).

---

<sup>†</sup> Electronic address: blumberg@uiuc.edu

[1] P.W. Anderson, *Science* **235**, 1196 (1987); P.W. Anderson and J.R. Schrieffer, *Physics Today* **44**(6), 54 (1991); the discussion by P.W. Anderson, D. Pines, and D.J. Scalapino, in *Physics Today* **47**(2), 9 (1994).

- [2] V.J. Emery, and S.A. Kivelson, *Phys. Rev. Lett.* **74**, 3253 (1995).
- [3] Y.J. Uemura *et al.*, *Phys. Rev. Lett.* **62**, 2317 (1989); Y.J. Uemura, in *Proc. of the Workshop on "Polarons and Bipolarons in High- $T_c$  Superconductors and Related Materials"*, Cambridge, UK, 1994, (eds by E.K.H. Salje *et al.*) 453-456 (Cambridge University Press, 1995).
- [4] M. Randeria, J.-M. Duan, and L.-Y. Shieh, *Phys. Rev. Lett.* **62**, 981 (1989); *Phys. Rev. B* **41**, 327 (1990).
- [5] V.J. Emery and S.A. Kivelson, *Nature*, **374**, 434 (1995); V.J. Emery, S.A. Kivelson, and O. Zachar, *Phys. Rev. B* **56**, 6120 (1997).
- [6] J. Schmalien, S. Grabowski, and K.H. Bennemann, *Phys. Rev. B* **56**, R509 (1997).
- [7] K.B. Lyons *et al.*, *Phys. Rev. Lett.* **60**, 732 (1988); S. Sugai, in *Springer Series in Materials Science* **11** (eds by Kamimura, H. and Oshiyama, A.) 207-219 (Springer-Verlag Berlin Heidelberg 1989).
- [8] G. Blumberg *et al.*, *Phys. Rev. B* **53**, R11 930 (1996); *SPIE Proceedings* **2696**, 205 (1996).
- [9] C.M. Varma *et al.*, *Phys. Rev. Lett.* **63**, 1996 (1989).
- [10] B.S. Shastry and B.I. Shraiman, *Phys. Rev. Lett.* **65**, 1068 (1990); *Intern. J. Mod. Phys. B* **5**, 365 (1991).
- [11] T. Staufer, R. Hackl, and P. Müller, *Solid State Comm.* **79**, 409 (1991); D. Reznik *et al.* *Phys. Rev. B* **46**, 11 725 (1992).
- [12] G. Blumberg *et al.*, *Phys. Rev. B* **49**, 13 295 (1994).
- [13] F. Slakey *et al.*, *Phys. Rev. B* **42**, 2643 (1990); C. Kendziora and A. Rosenberg, *Phys. Rev. B* **52**, R9867 (1995).
- [14] J. P. Rice and D. M. Ginsberg, *J. Cryst. Growth* **109**, 432 (1991); W. C. Lee and D. M. Ginsberg, *Phys. Rev. B* **44**, 2815 (1991).
- [15] B. W. Veal *et al.*, *Phys. Rev. B* **42**, 6305 (1990).
- [16] B. Dabrowski *et al.*, *Physica C* **202**, 271 (1992).
- [17] H. Ding *et al.*, *Nature*, **382**, 51 (1996).
- [18] C. Kendziora *et al.*, *Phys. Rev. B* **45**, 13 025 (1992); *Physica C* **257**, 74 (1996).
- [19] P. Guptasarma and D. Hinks, preprint.
- [20] M. Kang, G. Blumberg, M.V. Klein, and N.N. Kolesnikov, *Phys. Rev. Lett.* **77**, 4434 (1996).
- [21] T.P. Devereaux *et al.*, *Phys. Rev. Lett.* **72**, 396 (1994); *Phys. Rev. B* **51**, 16336 (1995); *Phys. Rev. B* **54**, 12523 (1996); D. Branch and J.P. Carbotte, *Phys. Rev. B* **52**, 603 (1995), and references therein.
- [22] M. Pressl *et al.*, *J. Raman Spectroscopy* **27**, 343 (1996).
- [23] F.C. Zhang and T.M. Rice, *Phys. Rev. B* **37**, 3759 (1988).
- [24] F. Slakey *et al.*, *Phys. Rev. B* **43**, 3764 (1991).
- [25] W.W. Warren *et al.*, *Phys. Rev. Lett.* **62**, 1193 (1989); R.E. Walstedt *et al.*, *Phys. Rev. B* **41**, 9574 (1990).
- [26] J. Rossat-Mignod *et al.*, *Physica B* **169**, 58 (1991); *ibid.* **186-188**, 1 (1993).
- [27] A.V. Puchkov, D.N. Basov, and T. Timusk, *J. Phys.: Condens. Matter* **8**, 10 049 (1996).
- [28] A.G. Loeser *et al.*, *Science* **273**, 325 (1996).
- [29] Ch. Renner *et al.*, submitted to *Phys. Rev. Lett.*